


EXPRESS LETTER

Open Access



# Space-to-space very low frequency radio transmission in the magnetosphere using the DSX and Arase satellites

James P. McCollough<sup>1,15</sup>, Yoshizumi Miyoshi<sup>2</sup>, Gregory P. Ginet<sup>3</sup>, William R. Johnston<sup>1\*</sup> , Yi-Jiun Su<sup>1</sup>, Michael J. Starks<sup>1</sup>, Yoshiya Kasahara<sup>4</sup>, Hirotsugu Kojima<sup>5</sup>, Shoya Matsuda<sup>6</sup>, Iku Shinohara<sup>7</sup>, Paul Song<sup>8</sup>, Bodo W. Reinisch<sup>8</sup>, Ivan A. Galkin<sup>8</sup>, Umran S. Inan<sup>9,10</sup>, David S. Lauben<sup>9</sup>, Ivan Linscott<sup>9</sup>, Alan G. Ling<sup>11</sup>, Shawn Allgeier<sup>3</sup>, Richard Lambour<sup>3</sup>, Jon Schoenberg<sup>3</sup>, William Gillespie<sup>3</sup>, Stephen Stelmash<sup>8</sup>, Kevin Roche<sup>8</sup>, Andrew J. Sinclair<sup>1</sup>, Jenny C. Sanchez<sup>1,16</sup>, Gregory F. Pedinotti<sup>12,13</sup> and Jarred T. Langhals<sup>1,14</sup>

## Abstract

Very low frequency (VLF) waves (about 3–30 kHz) in the Earth's magnetosphere interact strongly with energetic electrons and are a key element in controlling dynamics of the Van Allen radiation belts. Bistatic very low frequency (VLF) transmission experiments have recently been conducted in the magnetosphere using the high-power VLF transmitter on the Air Force Research Laboratory's Demonstration and Science Experiments (DSX) spacecraft and an electric field receiver onboard the Japan Aerospace Exploration Agency's Arase (ERG) spacecraft. On 4 September 2019, the spacecraft came within 410 km of each other and were in geomagnetic alignment. During this time, VLF signals were successfully transmitted from DSX to Arase, marking the first successful reception of a space-to-space VLF signal. Arase measurements were consistent with field-aligned propagation as expected from linear cold plasma theory. Details of the transmission event and comparison to VLF propagation model predictions are presented. The capability to directly inject VLF waves into near-Earth space provides a new way to study the dynamics of the radiation belts, ushering in a new era of space experimentation.

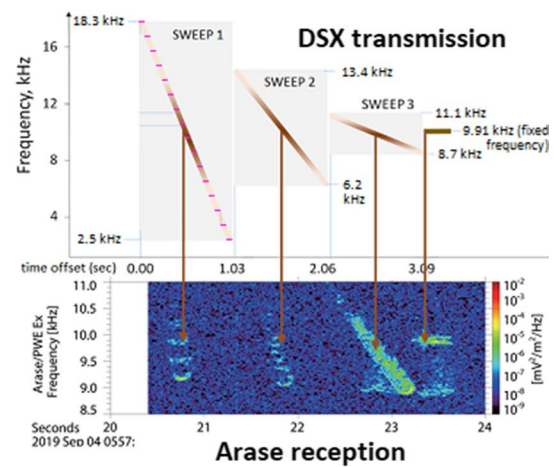
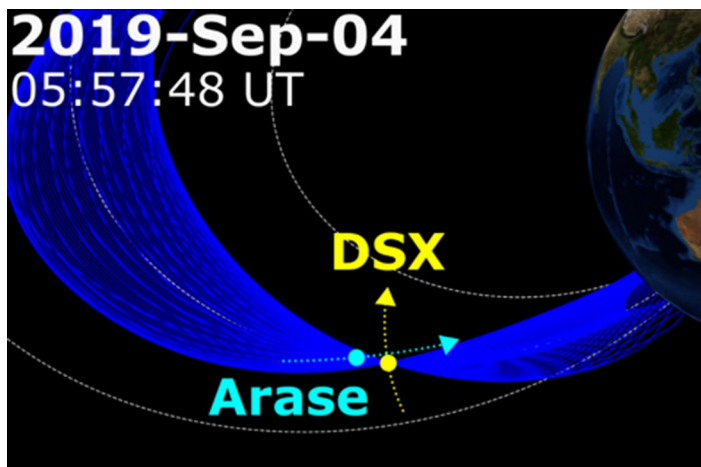
**Keywords:** Magnetosphere, VLF propagation, Active experiment, DSX, Arase

\*Correspondence: ae9ap9@vdl.afrl.af.mil

<sup>1</sup> Space Vehicles Directorate, Air Force Research Laboratory, Albuquerque, NM, Kirtland AFB, USA

Full list of author information is available at the end of the article

Graphical Abstract



Introduction

The Demonstration and Science Experiments (DSX) spacecraft, operated by the Air Force Research Laboratory, was launched on 25 June 2019 into Medium Earth Orbit (6000 km × 12,000 km × 42°) and operated through 31 May 2021. Outfitted with a very low frequency (VLF) radio transmitter, receiver, and full suite of energetic charged particle sensors, DSX’s primary science objective is to explore the influence of in situ VLF wave injection on energetic electrons in the Van Allen Radiation Belt (Scherbarth et al. 2009). It is well-established that VLF (~3–30 kHz) and extremely low frequency (ELF, ~3 Hz–3 kHz) waves can drive radiation belt electron accelerations and losses via resonant wave–particle interactions, including acceleration in the outer zone by ELF/VLF chorus, slot region losses from ELF plasmaspheric hiss, and slot region/outer zone losses from VLF waves generated by lightning or ground transmitters (Kennel and Petschek 1966; Lyons and Thorne 1973; Abel and Thorne 1998; Miyoshi et al. 2003, 2015, 2021). Here and throughout this work, we use the definitions of VLF and ELF ranges from Barr et al. (2000). DSX represents the first space-based mission to study the relationship by controlled injection of tailored VLF signals (Inan et al. 2003 and references therein). Establishing the radiation efficiency of an in situ VLF antenna is also an important step in estimating the performance of proposed space-based VLF radiation belt remediation systems (Winter et al. 2004; Carlsten et al. 2019) intended to protect satellites from high-energy electron damage.

One key activity to this end is to perform transmissions at times when the signal can be detected by a separate receiver in the far field, where near-field radiation efficiency and propagation phenomena determine the wave characteristics. In this bistatic mode the effects of top-side ionospheric or magnetospheric reflection are not present. Transmitting radio waves for the purposes of environmental observation has been performed in the past, including transmissions in the medium frequency band (300 kHz–3 MHz) between ISEE 1 and 2 (Harvey et al. 1988) and from the IMAGE spacecraft to the WIND and CLUSTER spacecraft (Cummer et al. 2003). These transmissions were in higher frequency bands where the requisite antenna length (at least in vacuo) is shorter than that required for VLF emission (3–30 kHz), and where propagation was nearly line-of-sight, i.e., at frequencies higher than the in situ plasma frequency and gyrofrequency. Two VLF transmission experiments were performed as part of the IMAGE mission (Song et al. 2007; Paznukhov et al. 2010). While these two experiments collected key engineering parameters, there was no confirmation that the waves propagated appreciably away from the satellite. Space-to-space VLF transmission was also previously attempted as part of the conjunction experiments between the Aktivny satellite and DE-1, but no signal was detected (Sonwalker et al. 1994). IMAGE Radio Plasma Imager also conducted VLF radio sounding experiments (Sonwalker et al. 2011) which received the echoes from the low-power whistler mode transmission. A novel aspect of DSX is that it utilizes a deployable rigid structure for the dipole antenna with a length of 81.6 m

and on-board tuning system which make high-driving-voltage and high-power transmission in the VLF band possible.

The DSX mission has attempted bistatic transmissions targeting several platforms which have the capability to receive signals in the VLF band, to include the Arase spacecraft operated by the Japan Aerospace Exploration Agency (JAXA). Arase has been performing magnetospheric observations since 2017 in a 460 km perigee, 32,110 km apogee and 31° inclination geosynchronous transfer orbit (Miyoshi et al. 2018a). In this paper, the first successful observation of a DSX VLF transmission by Arase is reported.

### Instrumentation and data collection

#### DSX

The DSX spacecraft consists of a payload module affixed to one side of an ESPA (Evolved Expendable Launch Vehicle Secondary Payload Adapter) bus and an avionics module on the opposite face as illustrated in Fig. 1a together with the spacecraft fixed coordinate frame. The primary VLF antenna has two 40 m booms used as an effective 81.6 m tip-to-tip dipole along the spacecraft Y-axis when the 1.6-m center gap is included. During the transmissions reported here, DSX maintained an

orientation relative to the geomagnetic field as shown (with +Y perpendicular to  $\mathbf{B}$ ). VLF studies are conducted with the Wave-Particles Interactions Experiment (WPIx) payload including a vector magnetometer built by the University of California at Los Angeles, an electron detector built by Boston University, a VLF broadband receiver (BBR) built by Stanford University and the Transmitter, Narrowband receiver, and Tuner (TNT) built by the University of Massachusetts at Lowell. The BBR is connected to orthogonal electric field antennas on the Y- and Z-booms (Fig. 1a) as well as to a three-axis flux-gate magnetometer built by NASA Goddard Spaceflight Center perched at the end of one of the Z-booms.

DSX performs VLF transmissions with the TNT which is composed of the two-element dipole antenna, cabling, a control unit and two sets of transmitters, receivers and tuning units (one for each antenna element). The instrument was designed with knowledge gained from the RPI instrument on the IMAGE spacecraft (Reinisch et al. 2000). All transmitted signals are derived from a 16-MHz system clock. A digital transmitter system generates desired frequencies in a time-series of waveforms with 5 V amplitude, then amplified to the transmitter driving voltage ranging from a few volts to more than 200 V. The transmitter is dynamically impedance matched to the

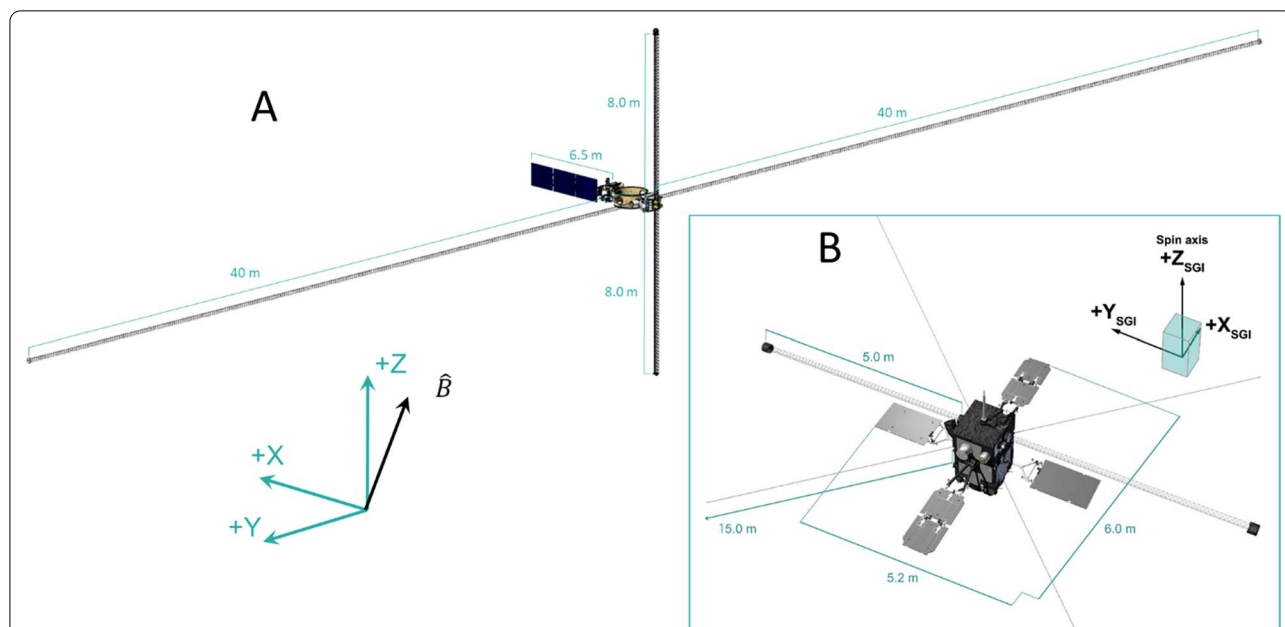


**Fig. 1** The DSX and Arase spacecraft and their fixed coordinate frames. **A** The DSX spacecraft consists of a payload module affixed to one side of an ESPA (Evolved Expendable Launch Vehicle Secondary Payload Adapter) bus and an avionics module on the opposite face. The VLF antenna has two 40 m booms used as an effective 80 m dipole along the spacecraft Y-axis. During transmission, DSX maintained an orientation relative to the geomagnetic field  $\mathbf{B}$  as shown (with +Y perpendicular to  $\mathbf{B}$ ). **B** The Arase spacecraft has a full suite of particle and field instruments for observing the inner magnetosphere. While DSX is 3-axis stabilized, Arase spins about its Z-axis as indicated in Spinning-satellite Geometry Inertia (SGI) coordinates

dipole polarized antenna feed points using a switched network of discrete inductors and capacitors with a total of 1024 different addressable values of net reactance. The narrow band receiver system passively records VLF electric field signals in 453 steps from 3 to 900 kHz with the reception bandwidth of 300 Hz.

The TNT system can broadcast in two modes—high power and low power. In the high-power mode, the payload transmits tuned signals at 3–50 kHz with up to 5 kV at the antenna feed points. For the high-power transmissions the impedance-matching network can either (a) maintain a fixed internal reactance while the VLF transmitter scans through frequencies to select the one which optimizes power flow to the antenna (at the resonance frequency) or (b) adjust the reactance to optimize the power flow at a fixed VLF transmit frequency. The dynamic impedance-matching maximizes power transfer from the TNT circuit to the dipole antenna as it encounters varying indices of refraction in the plasmasphere, radiation resistance and the reactance associated with local antenna–plasma interactions (Song et al. 2007; Paznukov et al. 2010). Low-power transmission modes are used for local and remote sounding by utilizing a frequency scan between 3 kHz and 3 MHz. For the sounding modes, the low-power antennas are not tuned. When the sounding frequency matches a local plasma characteristic frequency, resonance will occur and produce oscillations around the antenna. Such resonance relaxation sounding evaluates the local plasma frequency and gyrofrequency very accurately without altering underlying plasma properties. For frequencies which do not match a local resonant frequency, the pulsed signal propagates away and will reflect at locations where the frequency does match the local cutoff frequency and produce a reflection echo back to the satellite. Pulse travel times measured as a function of frequency provide information which can enable reconstruction of far-field plasmaspheric and polar cap density profiles along the magnetic field, as demonstrated by experiments on the IMAGE satellite (Reinisch et al. 2001).

#### **Arase**

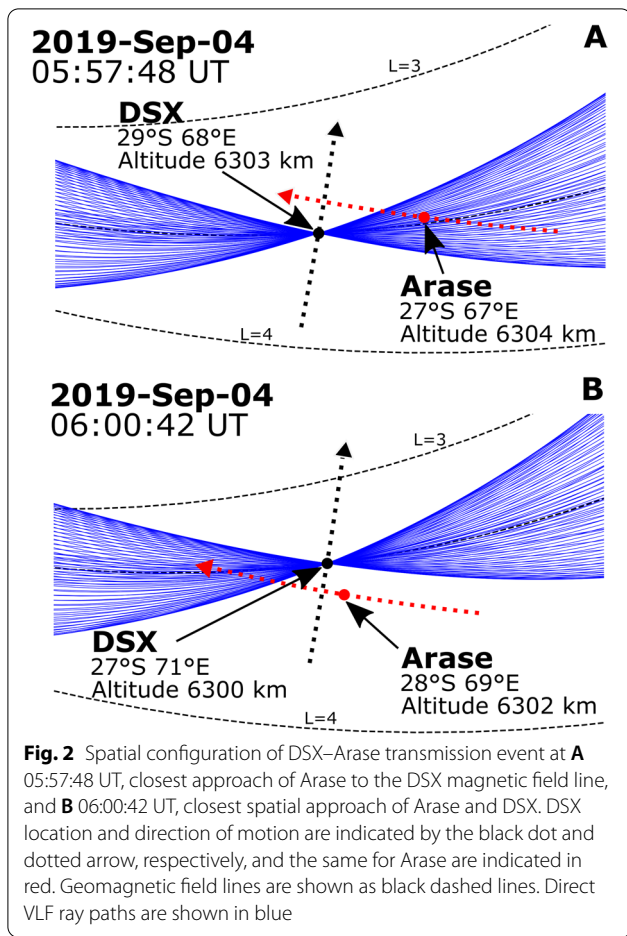
The Plasma Wave Experiment (PWE) aboard Arase measures electric and magnetic fields in the terrestrial inner magnetosphere (Kasahara et al. 2018) and comprises four electric field antennas (Wire Probe Antenna; WPT) to measure electric field (Kasaba et al. 2017), and a triaxial search coil magnetometer (MSC) to measure magnetic field (Ozaki et al. 2018). The length of each WPT is 15 m, and four WPTs are deployed in the spin plane of Arase as shown in Fig. 1B. MSC is mounted on the tip of a 5-m-long mast which is deployed from the spacecraft body. The PWE consists of three receivers: the Electric

Field Detector (EFD, Kasaba et al. 2017), the Waveform Capture/Onboard Frequency Analyzer (WFC/OFA, Matsuda et al. 2018), and the High Frequency Analyzer (HFA, Kumamoto et al. 2018). Using these three receivers, the PWE covers the frequency range from DC to 10 MHz for the electric field and from a few Hz to 100 kHz for the magnetic field.

The WFC/OFA measures electric and magnetic field in a frequency range from a few Hz to 20 kHz, with the WFC continuously sampling five components of the electric and magnetic field signals picked up by the PWE sensors at a sampling frequency of 65.536 kHz for limited periods of time. Electric and magnetic field spectra are generated onboard by the OFA using a fast Fourier transform with a nominal time resolution of 1 s. All OFA data are transferred to the ground. Waveforms observed by the WFC are stored once onto the onboard Mission Data Recorder and portions of the stored data are selected by telemetry commands and sent to ground. Since the WFC data represent uninterrupted high-resolution waveforms, that is what is used to observe DSX conjunction transmissions.

#### **DSX–Arase conjunctions**

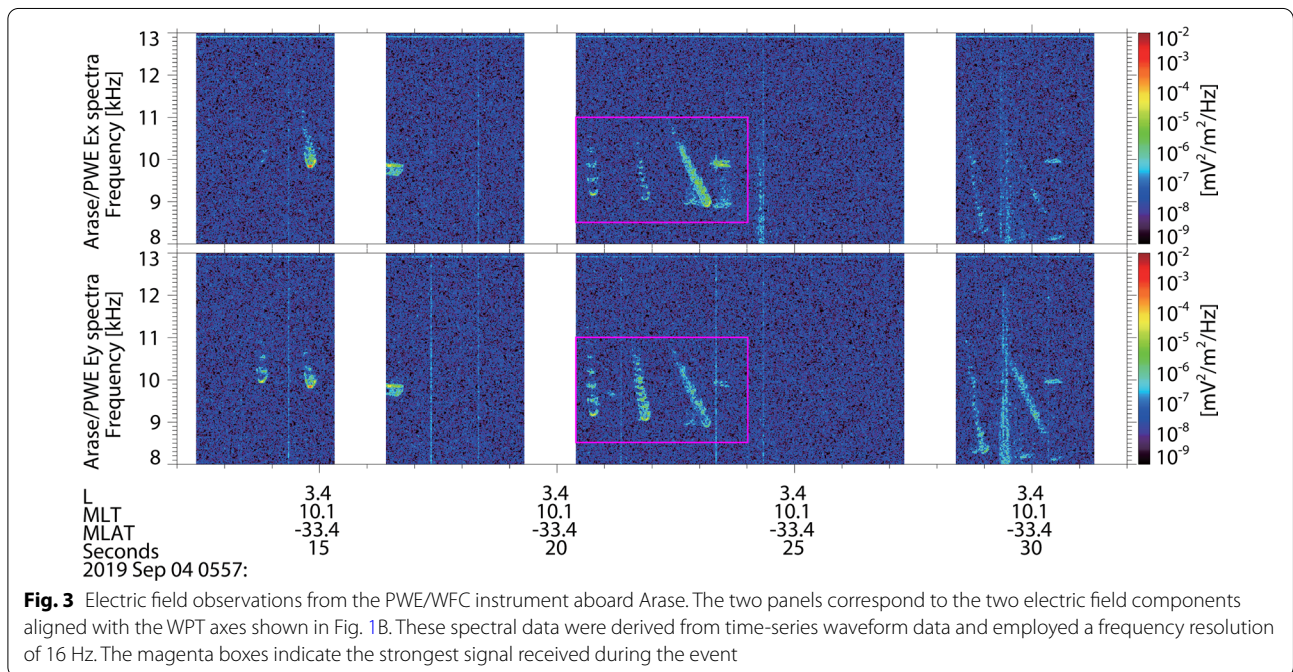
The DSX mission planning tools use spatial ephemerides for DSX and potential target spacecraft at a 1-min time resolution to identify two types of conjunctions: spatial and magnetic. Predicted spatial conjunctions are defined by physical separation between the two spacecraft of less than 2000 km, while predicted magnetic conjunctions are identified when the target spacecraft comes within 750 km in the transverse direction to the geomagnetic field line traced from DSX, though the distance along the magnetic field can be large. The DSX field line is traced using the International Geomagnetic Reference Field (IGRF) (Thébault et al. 2015) plus the Olson–Pfitzer quiet external field (Olson and Pfitzer 1974) both north and south from the predicted spacecraft location. Coordinated observations have been performed by the two satellite teams since August 2019, with Arase observing in burst mode to detect the waveform when DSX operates a high-power transmission. In the interval between 25 August 2019 and 31 December 2020 there were 17 conjunction events where the DSX transmitter specifically targeted Arase (see Additional file 1 and 2). Of these, 16 were field line conjunctions with spacecraft separation distances ranging from ~3040–24,225 km, and one has been a spatial conjunction with a separation distance of ~410 km. As described in the next section, a successful detection of the DSX signal by Arase occurred on 4 September 2019. This was the closest and only successful conjunction identified in data through the end of 2020.



**Results**

On 4 September 2019 DSX performed a transmission from 05:40 UT to 06:20 UT, centered about a closest approach to Arase of ~410 km at ~06:00:43 UT with wave power concentrated at ~10 kHz—the “whistler mode” in the context of cold plasma theory. Figure 2 shows the spatial configuration of this event as snapshots at A) 05:55 UT and B) 06:00 UT. The magnetic field measured by the vector magnetometer at 05:57:30 was ~3920 nT and the plasma number density determined from the measured upper-hybrid resonance detected with the low-power TNT sweep described above was ~390 cm<sup>-3</sup>.

Distinct electric field signatures that are qualitatively different from natural emissions or other known artificial sources (e.g., Barr et al. 2000) were recorded by the Arase PWE/WFC instrument (Fig. 3) between 05:57:15 and 05:57:30 UT according to the Arase spacecraft time. Here, L is the McIlwain L derived from the IGRF provided from the Arase Level-2 orbit files (Miyoshi et al. 2018b). At this time the spatial separation of DSX and Arase was ~1100 km, with both spacecraft located near the same geomagnetic field line (the transverse distance from the DSX field line to Arase was ~130 km and the distance along the DSX field line to the point of closest approach to Arase was ~1100 km), in agreement with established theory that whistler waves in the magnetosphere propagate primarily along magnetic field lines (Helliwell 1965). The entire period of signal reception spanned 05:57:06 to 05:58:39 UT, with closest approach of Arase to the DSX



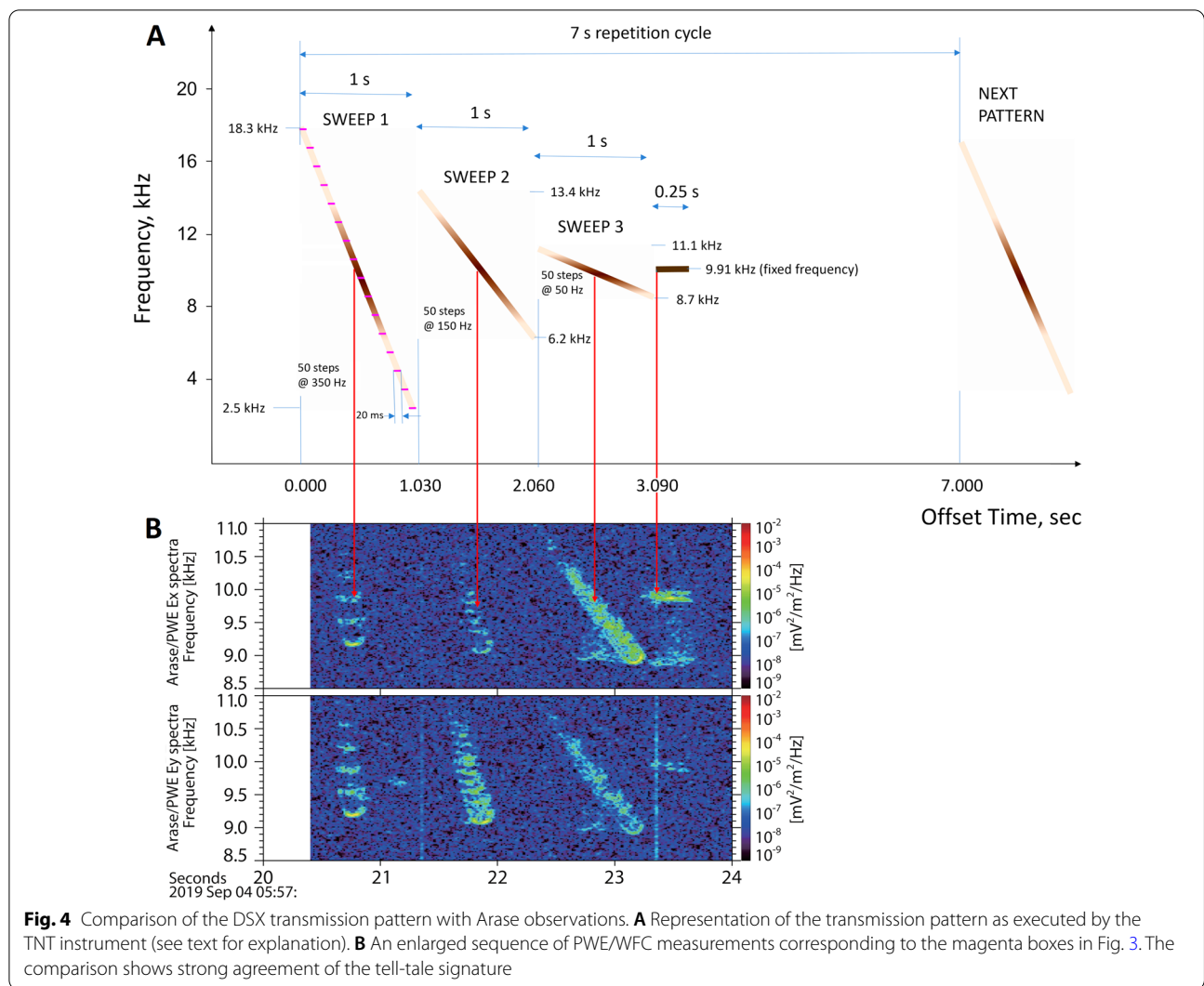


**Fig. 4** Comparison of the DSX transmission pattern with Arase observations. **A** Representation of the transmission pattern as executed by the TNT instrument (see text for explanation). **B** An enlarged sequence of PWE/WFC measurements corresponding to the magenta boxes in Fig. 3. The comparison shows strong agreement of the tell-tale signature

field line occurring at ~05:57:50 UT with ~112 km distance. Note that the closest spatial approach by the two spacecraft was at ~06:00:43 UT at ~410 km separation, but the distance between Arase and the DSX field line had increased to ~390 km. The precise timing of transmission and reception has relatively large uncertainty due to spacecraft clock drifts. The timing difference between the two spacecraft is within ~2 s.

The spatiotemporal and spectral characteristics of the observations in Fig. 3 agree with the operations of the transmitter. Figure 4 illustrates the DSX waveform during the conjunction with an enlarged sequence showing the Arase data from Fig. 3. TNT first scanned through the covered frequency range with a large frequency steps—50 steps at 350 Hz each (shown as short magenta dashes in Fig. 4A; only a subset of actual frequency steps are shown for clarity). From the measured antenna voltages, an approximate tuned frequency was identified.

TNT then performs an intermediate-step (50 steps with 150 Hz each) and a fine-step (50 steps with 50 Hz each) frequency scan about the approximate tuned frequency. From these three frequency scans (each 1 s long) TNT locked in the final tuned frequency at 9.91 kHz for a long pulse (0.25 s) high-power transmission. Shades of brown color are used to indicate varying TNT power at different frequencies in the sweeps: transmissions are stronger in the vicinity of the resonance frequency. The whole transmission cycle repeats every 7 s. Relative timing of the measured spacecraft signal in Fig. 4 is in close agreement with the DSX waveform and the spectral features conform, providing strong evidence that this signal from DSX was detected by Arase. A total of 3 such transmission cycles in sequence were detected by Arase over the 40 min high-power transmission period.

The measurements are qualitatively consistent with results from the baseline DSX wave injection and

propagation model based on VLF ray-tracing—a computationally efficient geometric optics approach amenable to anisotropic media that works well when the wavelength of interest is larger than the scale of variations in the medium. This condition is generally valid for the DSX orbit. Raytracing starts with a model to estimate the propagating wave vectors and Poynting flux injected into the magnetosphere from an in situ dipole antenna. The model employs the stationary phase, far-field approximation to obtain a solution to the Green's function for the electric and magnetic fields driven by the antenna current in the limit of cold-plasma linear response theory (Mitra and Deschamps 1963; Ginat 2020). Estimates of the wave vectors and Poynting flux are output on the surface of a sphere of constant radius (100 km) assuming a homogeneous plasma. Variations in the background density and magnetic field on the surface are then accounted for by adjusting the wave vectors using local density and magnetic field conditions constrained so that the adjusted wave vector is in the plane of the magnetic field and original wave vector. At this time, the predictions of Poynting flux amplitude are only relative. The antenna performance is still being evaluated and consistent values for the antenna impedance and current required for quantitative flux estimates are not yet available.

Initial conditions on the sphere are then fed into the magnetospheric ray-tracing model (Starks et al. 2008) to produce estimates of the ray paths and Poynting flux as a function of location and group delay. The model includes divergence, focusing and damping effects and represents the Earth's magnetic field by a tilted offset dipole model based on the first eight Gauss coefficients from IGRF. The ambient plasma environment is given by a multi-species diffusive equilibrium density model described in Sect. 2.3 of Starks et al. (2008). No field-aligned ducts are included in the ray-tracing.

VLF ray paths for the DSX–Arase conjunction predicted by the baseline propagation model described above are shown in Fig. 2. Energy propagating directly from DSX to Arase is shown in blue. Arase begins intersecting the direct wave power around this time, in agreement with observations. These paths serve as a qualitative guide for interpreting spacecraft data; detailed model/data comparison is ongoing and when complete should provide more quantitative information on the properties of the emitted VLF waves (e.g., Sonwalker et al. 2001).

## Conclusions

This result represents the first reported successful bistatic space-to-space transmission of VLF waves in the magnetosphere. It establishes the ability of an in situ antenna to transmit VLF wave power into the far field with potential applications for controlled studies of wave–particle interactions and radiation belt remediation. The

spatial location and temporal variation of the electric fields measured by Arase are consistent with the radiation pattern expected from cold plasma theory, i.e., a narrow cone along the magnetic field, and clearly inconsistent with a standard dipole radiation pattern in vacuo.

Of the 17 DSX–Arase conjunction transmission attempts through the end of 2020, only one appears to be successful. This is likely due to the proximity of the satellites during the 04 September 2019 event together with the very narrow radiation cone and anisotropic nature of VLF propagation in the magnetosphere. However, DSX has conducted a large number of successful sounding experiments where TNT transmitted pulses which have undergone magnetospheric reflection (Kimura 1966), returned to the spacecraft and were detected by the BBR. Conjunction and sounding experiments continued through the end of mission on 31 May 2021. Together with ongoing analysis of the TNT transmitter impedance, the BBR response and the VLF propagation model, the data are expected to provide a quantitative understanding of the dipole antenna far-field injection efficiency and subsequent propagation effects.

## Abbreviations

BBR: Broad band receiver; DE-1: Dynamics Explorer 1; DSX: Demonstration and Science Experiments; EFD: Electric Field Detector; ELF: Extremely low frequency; ERG: Energization and radiation in geospace; ESPA: Evolved Expendable Launch Vehicle Secondary Payload Adapter; HFA: High Frequency Analyzer; IGRF: International Geomagnetic Reference Field; IMAGE: Imager for Magnetopause-to-Aurora Global Exploration; ISEE: International Sun Earth Explorer; MSC: Triaxial search coil magnetometer; PWE: Plasma Wave Experiment; RPI: Radio Plasma Imager; SPDF: Space Physics Data Facility; SGI: Spinning-satellite Geometry Inertia; TNT: Transmitter, Narrowband receiver, and Tuner; VLF: Very low frequency; WFC/OFA: Waveform Capture/Onboard Frequency Analyzer; WPT: Wire Probe Antenna.

## Supplementary Information

The online version contains supplementary material available at <https://doi.org/10.1186/s40623-022-01605-6>.

**Additional file 1:** DSX–ARASE magnetic field line conjunction characteristics. Perpendicular distance from the DSX field line to the Arase satellite at point of closest approach vs. distance along the DSX field line from the DSX satellite to the point of closest approach for the 17 conjunction events.

**Additional file 2:** Parameters for the 17 DSX–Arase conjunction events. Description: DSX–Arase conjunction parameters are as follows: Start\_Time (UTC) = start time of the high-power transmission event. Duration (min) = duration of the high-power transmission event. Frequency (Hz) = frequency of the transmission. Lm\_min = minimum McIlwain L-shell reached during the event. Lm\_max = maximum McIlwain L-shell reached during the event. MLT\_start (hr) = magnetic local time at the start of the event. MLT\_stop (hr) = magnetic local time at the end of the event. MLAT\_min (deg) = minimum magnetic latitude reached during the event. MLAT\_max (deg) = maximum magnetic latitude reached during the event. Phys\_Dist\_min (km) = minimum separation distance between the DSX and Arase satellites reached during the event. FL\_Perp\_min (km) = minimum perpendicular distance between the DSX magnetic field line and Arase satellite reached during the event. FL\_Parallel (km) = distance along the DSX field line between the DSX satellite and the point at which FL\_Perp is minimum during the event.

### Acknowledgements

The DSX team acknowledges S.A. Reames, K.E. Carey, C.M. Straight, E.A. Kent, and the DSX Operations Cadre and Mission Planning Team for their role in making this event possible, and J.S. Christmas and R.K. Delaney for program support. We also thank S.M. O'Malley, I. Vlad, and C. Roth for support in data processing and analysis.

### Authors' contributions

JM and GG conceptualized and supervised the DSX experiment supported by PS, BR, and UI. YM and IS conceptualized the Arase experiment. WJ and YJS performed DSX data curation. JM, GG, WJ, YJS, MS, PS, IG, DL, AL, AS, and JL performed DSX analysis. AL, SA, and AS produced software for DSX analysis. YM, YK, HK, SM, and IS performed Arase analysis. SA, RL, JS, SS, KR, and GP provided DSX resources. RL and WG performed DSX data validation. IS performed Arase administration and WG, JCS performed DSX administration. JM, YM, and PS wrote the paper with contributions from GG, WJ, YJS, MS, YK, HK, SM, IS, BR, IG, UI, DL, IL, SA, RL, AS, JCS, JS, and JL. All authors read and approved the final manuscript.

### Funding

DSX research and operations are funded by the Air Force Research Laboratory's Space Vehicles Directorate including contracts FA9453-19-C-0057 (Stanford Univ.), FA9453-19-C-0056 (Univ. of Mass. Lowell), and FA8702-15-D-0001 (MIT Lincoln Laboratory). Arase elements of this study are supported by Grants-in-Aid-for Scientific Research (15H05815, 16H06286, 16H04056, 16H01172, 17H00728, 17H06140, 18H04441, 20H01959, 20K14546) of Japan Society for the Promotion of Science (JSPS).

### Availability of data and materials

The event times, DSX position, Arase–DSX separation distance and transmitting frequency bands for the DSX–Arase conjunction experiments are contained in Additional file 2: Table S1. DSX science data will be available through the NASA Space Physics Data Facility (SPDF) in summer 2022 (estimated). Science data of the ERG (Arase) satellite were obtained from the ERG Science Center operated by ISAS/JAXA and ISEE/Nagoya University (<https://ergsc.isee.nagoya-u.ac.jp/index.shtml>), Miyoshi et al. 2018c). In the present study, level-2 PWE/WFC waveform v00.01 data (Kasahara et al. 2020) and level-2 obt (Miyoshi et al. 2018b) were used.

### Declarations

#### Ethics approval and consent to participate

Not applicable.

#### Consent for publication

Not applicable.

#### Competing interests

The authors declare that they have no competing interests.

#### Author details

<sup>1</sup>Space Vehicles Directorate, Air Force Research Laboratory, Albuquerque, NM, Kirtland AFB, USA. <sup>2</sup>Institute for Space-Earth Environmental Research, Nagoya University, Nagoya, Japan. <sup>3</sup>MIT Lincoln Laboratory, Lexington, MA, USA. <sup>4</sup>Kanazawa University, Kanazawa, Japan. <sup>5</sup>Kyoto University, Uji, Japan. <sup>6</sup>Graduate School of Natural Science and Technology, Kanazawa University, Kanazawa, Japan. <sup>7</sup>Institute of Space and Astronautical Science, Japan Aerospace Exploration Agency, Sagami, Japan. <sup>8</sup>Space Science Laboratory, University of Massachusetts Lowell, Lowell, MA, USA. <sup>9</sup>Department of Electrical Engineering, Stanford University, Palo Alto, CA, USA. <sup>10</sup>Department of Electrical Engineering, Koç University, Istanbul, Turkey. <sup>11</sup>Atmospheric and Environmental Research, Inc, Albuquerque, NM, USA. <sup>12</sup>ATA Aerospace, Albuquerque, NM, USA. <sup>13</sup>Present Address: MEI Technologies, Albuquerque, NM, USA. <sup>14</sup>Present Address: Innovation and Prototyping Directorate, Space Systems Command, Albuquerque, NM, Kirtland AFB, USA. <sup>15</sup>Present Address: U.S. Department of Energy, Albuquerque, NM, USA. <sup>16</sup>Present Address: Space Systems Command, Albuquerque, NM, Kirtland AFB, USA.

Received: 2 December 2021 Accepted: 8 March 2022

Published online: 27 April 2022

### References

- Abel B, Thorne RM (1998) Electron scattering loss in Earth's inner magnetosphere: 1. Dominant physical processes. *J Geophys Res* 103(A2):2397–2407. <https://doi.org/10.1029/97JA02920>
- Barr R, Jones DL, Rodger CJ (2000) ELF and VLF radio waves. *J Atmos Sol Terr Phys* 62:1689–1718. [https://doi.org/10.1016/S1364-6826\(00\)00121-8](https://doi.org/10.1016/S1364-6826(00)00121-8)
- Carlsten BE, Colestock PL, Cunningham GS, Delzanno GL, Dors EE, Holloway MA et al (2019) Radiation-belt remediation using space-based antennas and electron beams. *IEEE Trans Plasma Sci* 47(5):2045–2063. <https://doi.org/10.1109/TPS.2019.2910829>
- Cummer SA, Green JL, Reinisch BW, Fung SF, Kaiser ML, Pickett JS et al (2003) Advances in magnetospheric radio wave analysis and tomography. *Adv Space Res* 32:329–336. [https://doi.org/10.1016/S0273-1177\(03\)00270-9](https://doi.org/10.1016/S0273-1177(03)00270-9)
- Ginet GP (2020) VLF far-field radiation from a linear dipole immersed in a plasma: Baseline model for DSX. MIT Lincoln Laboratory Report 95–002, DTIC #AD1103378, Lexington, MA
- Harvey CC, Celnikier L, Hubert D (1988) Results from the ISEE propagation density experiment. *Adv Space Res* 8:185–196. [https://doi.org/10.1016/0273-1177\(88\)90131-7](https://doi.org/10.1016/0273-1177(88)90131-7)
- Helliwell RA (1965) Whistlers and related ionospheric phenomena. Stanford University Press, Stanford
- Inan US, Bell TF, Bortnik J, Albert JM (2003) Controlled precipitation of radiation belt electrons. *J Geophys Res* 108:1186. <https://doi.org/10.1029/2002J1A009580>
- Kasaba Y, Ishisaka K, Kasahara Y, Imachi T, Yagitani S, KojimaMatsuda HS et al (2017) Wire probe antenna (WPT) and electric field detector (EFD) of plasma wave experiment (PWE) aboard the Arase satellite: specifications and initial evaluation results. *Earth Planets Space* 69:174. <https://doi.org/10.1186/s40623-017-0760-x>
- Kasahara Y, Kasaba Y, Kojima H, Yagitani S, Ishisaka K, Kumamoto A et al (2018) The plasma wave experiment (PWE) on board the Arase (ERG) satellite. *Earth Planets Space* 70:86. <https://doi.org/10.1186/s40623-018-0842-4>
- Kasahara Y, Kojima H, Matsuda S, Shoji M, Nakamura S, Kitahara M, Shinohara I, Miyoshi Y (2020) The PWE/WFC instrument Level-2 electric field data of Exploration of Energization and Radiation in Geospace (ERG) Arase satellite, Version v00\_01. ERG Science Center, Institute for Space-Earth Environmental Research, Nagoya University, Nagoya. <https://doi.org/10.34515/DATA.ERG-09002>
- Kennel CF, Petschek HE (1966) Limit on stably trapped particle fluxes. *J Geophys Res* 71:1. <https://doi.org/10.1029/JZ071i001p00001>
- Kimura I (1966) Effects of ions on whistler-mode ray tracing. *Radio Sci* 1:269–283. <https://doi.org/10.1002/rds196613269>
- Kumamoto A, Tsuchiya F, Kasahara Y, Kasaba Y, Kojima H, Yagitani S et al (2018) High frequency analyzer (HFA) of plasma wave experiment (PWE) onboard the Arase spacecraft. *Earth Planets Space* 70:82. <https://doi.org/10.1186/s40623-018-0854-0>
- Lyons LR, Thorne RM (1973) Equilibrium structure of the radiation belt electrons. *J Geophys Res* 78:2142. <https://doi.org/10.1029/JA078i013p02142>
- Matsuda S, Kasahara Y, Kojima H, Kasaba Y, Yagitani S, Ozaki M et al (2018) Onboard software of plasma wave experiment aboard Arase: instrument management and signal processing of waveform capture/onboard frequency analyzer. *Earth Planets Space* 70:75. <https://doi.org/10.1186/s40623-018-0838-0>
- Mitra R, Deschamps GA (1963) Field solution for a dipole in a cold anisotropic medium. In: Jordan EC (ed) Symposium on electromagnetic theory and antennas, part 1. Pergamon Press, New York, pp 495–512
- Miyoshi Y, Obara T, Misawa H, Nagai T, Kasahara Y (2003) Rebuilding process of the outer radiation belt during the November 3, 1993, magnetic storm: NOAA and EXOS-D observations. *J Geophys Res* 108(A1):1004. <https://doi.org/10.1029/2001JA007542>
- Miyoshi Y, Oyama S, Saito S, Kurita S, Fujiwara H, Kataoka R et al (2015) Energetic electron precipitation associated with pulsating aurora: EISCAT and Van Allen probes observations. *J Geophys Res* 120:2754–2766
- Miyoshi Y, Shinohara I, Takashima T, Asamura K, Higashio N, Mitani T et al (2018a) Geospace Exploration Project ERG. *Earth Planets Space* 70:101. <https://doi.org/10.1186/s40623-018-0862-0>
- Miyoshi Y, Shinohara I, Jun C-W (2018b) The level-2 orbit data of exploration of energization and radiation in geospace (ERG) Arase satellite, version v03. ERG Science Center, Institute for Space-Earth Environmental Research, Nagoya University, Nagoya. <https://doi.org/10.34515/DATA.ERG-12000>



- Miyoshi Y, Hori T, Shoji M, Teramoto M, Chang TF, Segawa T et al (2018c) The ERG science center. *Earth Planets Space* 70:96. <https://doi.org/10.1186/s40623-018-0867-8>
- Miyoshi Y, Hosokawa K, Kurita S, Oyama S-I, Ogawa Y, Saito S, Shinohara I, Kero A, Turunen E, Verronen PT, Kasahara S, Yokota S, Mitani T, Takashima T, Higashio N, Kasahara Y, Masuda S, Tsuchiya F, Kumamoto A, Matsuoka A, Hori T, Keika K, Shoji M, Teramoto M, Imajo S, Jun C, Nakamura S (2021) Penetration of MeV electrons into the mesosphere accompanying pulsating aurorae. *Sci Rep* 11:13724. <https://doi.org/10.1038/s41598-021-92611-3>
- Olson WP, Pfitzer KA (1974) A quantitative model of the magnetospheric magnetic field. *J Geophys Res* 79:3739. <https://doi.org/10.1029/JA079i025p03739>
- Ozaki M, Yagitani S, Kasahara Y, Kojima H, Kasaba Y et al (2018) Magnetic search coil (MSC) of plasma wave experiment (PWE) aboard the Arase (ERG) satellite. *Earth Planets Space*. <https://doi.org/10.1186/s40623-018-0837-1>
- Paznukhov VV, Sales GS, Bibl K, Reinisch BW, Song P, Huang X, Galkin I (2010) Impedance characteristics of an active transmitting antenna radiating in the whistler mode. *J Geophys Res* 115:A09212. <https://doi.org/10.1029/2009JA014889>
- Reinisch BW, Haines DM, Bibl K, Cheney G, Galkin IA, Huang X et al (2000) The radio plasma imager investigation on the IMAGE spacecraft. *Space Sci Rev* 91:319–359. <https://doi.org/10.1023/A:1005252602159>
- Reinisch BW, Huang X, Song P, Sales GS, Fung SF, Green JL et al (2001) Plasma density distribution along the magnetospheric field: RPI observations from IMAGE. *Geophys Res Lett* 28:4521–4524. <https://doi.org/10.1029/2001GL013684>
- Scherbarth M, Smith D, Adler A, Stuart J, Ginet GP (2009) AFRL's demonstration and science experiments (DSX) mission. In: Fineschi S, Fennelly JA (eds) *Solar physics and space weather instrumentation III* Proceeding of SPIE. The International Society for Optical Engineering, Bellingham, p 7438
- Song P, Reinisch BW, Paznukhov V, Sales G, Cooke D, Tu JN et al (2007) High voltage antenna-plasma interaction in whistler wave transmission: plasma sheath effects. *J Geophys Res* 112:A03205. <https://doi.org/10.1029/2006JA011683>
- Sonwalkar VS, Inan US, Bell TF, Helliwell RA, Molchanov OA, Green JL (1994) DE 1 VLF observations during activity wave injection experiments. *J Geophys Res* 99(A4):6173–6186. <https://doi.org/10.1029/93JA03310>
- Sonwalkar VS, Chen X, Harikumar J, Carpenter DL, Bell TF (2001) Whistler-mode wave-injection experiments in the plasmasphere with a radio sounder. *J Atmos Sol Terr Phys* 63:1199–1216. [https://doi.org/10.1016/S1364-6826\(00\)00223-6](https://doi.org/10.1016/S1364-6826(00)00223-6)
- Sonwalkar VS, Carpenter DL, Reddy A, Proddaturi R, Hazra S, Mayank K, Reinisch BW (2011) Magnetically reflected, specularly reflected, and backscattered whistler mode radio-sounder echoes observed on the IMAGE satellite: 1. Observations and Interpretation. *J Geophys Res* 116:A11210. <https://doi.org/10.1029/2011JA016759>
- Starks MJ, Quinn RA, Ginet GP, Albert JM, Sales GS, Reinisch BW, Song P (2008) Illumination of the plasmasphere by terrestrial very low frequency transmitters: model validation. *J Geophys Res* 113:A09320. <https://doi.org/10.1029/2008JA013112>
- Thébault E, Finaly CC, Beggan CD, Alken P, Aubert J, Barrois O et al (2015) International geomagnetic reference field: the 12th generation. *Earth Planets Space* 67:79. <https://doi.org/10.1186/s40623-015-0228-9>
- Winter J, Spanjers G, Cohen D, Adler A, Ginet G, Dichter B et al (2004) A proposed large deployable space structures experiment for high power, large aperture missions in MEO. In: IEEE aerospace conference (IEEE Cat. No.04TH8720) 2004. IEEE, New York, pp 525–532. <https://doi.org/10.1109/AERO.2004.1367636>

## Publisher's Note

Springer Nature remains neutral with regard to jurisdictional claims in published maps and institutional affiliations.

Submit your manuscript to a SpringerOpen® journal and benefit from:

- Convenient online submission
- Rigorous peer review
- Open access: articles freely available online
- High visibility within the field
- Retaining the copyright to your article

Submit your next manuscript at ► [springeropen.com](https://www.springeropen.com)